



**HAL**  
open science

## Tiled QR factorization algorithms

Henricus Bouwmeester, Mathias Jacquelin, Julien Langou, Yves Robert

► **To cite this version:**

Henricus Bouwmeester, Mathias Jacquelin, Julien Langou, Yves Robert. Tiled QR factorization algorithms. [Research Report] RR-7601, 2011. inria-00585721v2

**HAL Id: inria-00585721**

**<https://inria.hal.science/inria-00585721v2>**

Submitted on 15 Apr 2011 (v2), last revised 22 Apr 2011 (v3)

**HAL** is a multi-disciplinary open access archive for the deposit and dissemination of scientific research documents, whether they are published or not. The documents may come from teaching and research institutions in France or abroad, or from public or private research centers.

L'archive ouverte pluridisciplinaire **HAL**, est destinée au dépôt et à la diffusion de documents scientifiques de niveau recherche, publiés ou non, émanant des établissements d'enseignement et de recherche français ou étrangers, des laboratoires publics ou privés.



INSTITUT NATIONAL DE RECHERCHE EN INFORMATIQUE ET EN AUTOMATIQUE

## *Tiled QR factorization algorithms*

Henricus Bouwmeester — Mathias Jacquelin — Julien Langou — Yves Robert

**N° 7601**

Avril 2011

Distributed and High Performance Computing



*R*  
*apport*  
*de recherche*



## Tiled QR factorization algorithms

Henricus Bouwmeester<sup>\*†</sup>, Mathias Jacquelin<sup>‡</sup>, Julien Langou<sup>\*§</sup>,  
Yves Robert<sup>‡¶||</sup>

Theme : Distributed and High Performance Computing  
Équipe-Projet GRAAL

Rapport de recherche n° 7601 — Avril 2011 — 26 pages

**Abstract:** This work revisits existing algorithms for the QR factorization of rectangular matrices composed of  $p \times q$  tiles, where  $p \geq q$ . Within this framework, we study the critical paths and performance of algorithms such as SAMEH-KUCK, FIBONACCI, GREEDY, and those found within PLASMA. Although neither FIBONACCI nor GREEDY is optimal, both are shown to be asymptotically optimal for all matrices of size  $p = q^2 f(q)$ , where  $f$  is any function such that  $\lim_{+\infty} f = 0$ . This novel and important complexity result applies to all matrices where  $p$  and  $q$  are proportional,  $p = \lambda q$ , with  $\lambda \geq 1$ , thereby encompassing many important situations in practice (least squares). We provide an extensive set of experiments that show the superiority of the new algorithms for tall matrices.

**Key-words:** QR factorization, critical path, greedy algorithms, tall and skinny

\* University of Colorado Denver

† Research of the first author was fully supported by the National Science Foundation grant # NSF CCF 811520.

‡ École Normale Supérieure de Lyon

§ Research of the third author was fully supported by the National Science Foundation grant # NSF CCF 1054864.

¶ Institut Universitaire de France

|| Research of the fourth author was supported in part by the ANR StochaGrid and RES-CUE projects.

## Algorithmes de factorisation QR par blocs

**Résumé :** Cette étude revisite les algorithmes existant pour la factorisation QR de matrices rectangulaires composées de  $p \times q$  blocs, où  $p \geq q$ . Dans ce contexte, nous étudions les chemins critiques et les performances d'algorithmes tels que SAMEH-KUCK, FIBONACCI, GREEDY, ainsi que ceux disponibles dans PLASMA. Bien que ni FIBONACCI ni GREEDY ne soient optimaux, nous démontrons qu'ils sont tous deux asymptotiquement optimaux pour toute matrice de taille  $p = q^2 f(q)$ , où  $f$  est une fonction quelconque telle que  $\lim_{+\infty} f = 0$ . Ce résultat est valide pour toute matrice dès lors que  $p$  et  $q$  sont proportionnels,  $p = \lambda q$ , avec  $\lambda \geq 1$ , comprenant par là même de nombreuses situations importantes rencontrées en pratique (moindre carrés). Nous présentons un grand nombre d'expériences mettant en exergue la supériorité des nouveaux algorithmes pour les matrices ayant significativement plus de lignes que de colonnes.

**Mots-clés :** Factorisation QR, chemin critique, algorithmes gloutons, matrice ayant significativement plus de lignes que de colonnes

## 1 Introduction

Given an  $m$ -by- $n$  matrix  $A$  with  $n \leq m$ , we consider the computation of its QR factorization, which is the factorization  $A = QR$ , where  $Q$  is an  $m$ -by- $n$  unitary matrix ( $Q^H Q = I_n$ ), and  $R$  is upper triangular.

The QR factorization is the time consuming stage of some important numerical computations. The QR factorization of an  $m$ -by- $n$  matrix with  $n \leq m$  is needed for solving a linear least squares with  $m$  equations (observations) and  $n$  unknowns. The QR factorization of an  $m$ -by- $n$  matrix with  $n \leq m$  is used to compute an orthogonal basis (the  $Q$ -factor) of the column span of the initial matrix  $A$ . For example, all block iterative methods (used to solve large sparse linear systems of equations or computing some relevant eigenvalues of such systems) require orthogonalizing a set of vectors at each step of the process. For these two usage examples, while  $n \leq m$ ,  $n$  can range from  $n \ll m$  to  $n \approx m$ . We note that the extreme case  $n = m$  is also relevant: the QR factorization of a matrix can be used to solve (square) linear systems of equations (in that case  $n = m$ ). While this requires twice as many flops as an LU factorization, using a QR factorization (a) is unconditionally stable (Gaussian elimination with partial pivoting or pairwise pivoting is not) and (b) avoids pivoting so it may well be faster in some cases (despite requiring twice as many flops).

To obtain a QR factorization, we consider algorithms which apply a sequence of  $m$ -by- $m$  unitary transformations,  $U_i$ , ( $U_i^H U_i = I$ ),  $i = 1, \dots, \ell$ , on the left of the matrix  $A$ , such that after  $\ell$  transformations the resulting matrix  $R = U_\ell \dots U_1 A$  is upper triangular, in which case,  $R$  is indeed the  $R$ -factor of the QR factorization. The  $Q$ -factor (if needed) can then be obtained by computing  $Q = U_1^H \dots U_\ell^H$ . These types of algorithms are in regular use, e.g. in the LAPACK and ScaLAPACK libraries, and are favored over others algorithms (Cholesky QR or Gram-Schmidt) for their stability.

The unitary transformation  $U_i$  is chosen so as to introduce some zeros in the current update matrix  $U_{i-1} \dots U_1 A$ . The two basic transformations are Givens rotations and Householder reflections. One Givens rotation introduces one additional zero; the whole triangularization requires  $mn - n(n+1)/2$  Givens rotations for  $n < m$ . One elementary Householder reflection simultaneously introduces  $m-i$  zeros in position  $i+1$  to  $m$  in column  $i$ ; the whole triangularization requires  $n$  Householder reflections for  $n < m$ . (See LAPACK subroutine *GEQR2*.) The LAPACK *GEQRT* subroutine constructs a compact WY representation to apply a sequence of  $ib$  Householder reflections, this enables one to introduce the appropriate zeros in  $ib$  consecutive columns and thus leverage optimized Level 3 BLAS subroutines during the update. The blocking of Givens rotations is also possible but is more costly in terms of flops.

The main interest of Givens rotations over Householder transformations is that one can concurrently introduce zeros using disjoint pairs of rows, in other words, two transformations  $U_i$  and  $U_{i+1}$  may be applicable concurrently. This is not possible using the original Householder reflection algorithm since the transformations work on whole columns and thus does not exhibit this type of intrinsic parallelism forcing this kind of Householder reflections to be applied sequentially. The advantage of Householder reflections over Givens rotations is that, first, Householder reflections perform less flops, and second, the compact WY transformation enables high sequential performance of the algorithm. In a multicore setting, where data locality and parallelism are crucial algorithmic

characteristics for enabling performance, the tiled QR factorization algorithm combines both ideas: use of Householder reflections for high sequential performance and use of a scheme ala Givens rotations to enable parallelism within cores. In essence, one can think (i) either of the tiled QR factorization as a Givens rotation scheme but on tiles ( $m_b$ -by- $n_b$  submatrices) instead of on scalars (1-by-1 submatrices) as in the original scheme, (ii) or of it as a blocked Householder reflection scheme where each reflection is confined to an extent much less than the full column span, which enables concurrency with other reflections.

Tiled QR factorization in the context of multicore architectures has been introduced in [4, 13, 5]. Initially the focus was on square matrices and the sequence of unitary transformations presented was analogous to SAMEH-KUCK [14], which corresponds to reducing the panels with flat trees. The use of binary trees for tall and skinny matrices is explained in [8]. In [10], Hadri et al. propose to combine flat trees and binary trees to handle the intermediate cases. Our theoretical and experimental work explains that we can adapt FIBONACCI [12] and GREEDY [6, 7] to tiles, resulting in better algorithms.

The sequential kernels of the Tiled QR factorization (executed on a core) are made of standard blocked algorithms ala LAPACK encoded in kernels; the development of these kernels is well understood. The focus of this paper is on improving the overall degree of parallelism of the algorithm. Given a  $p$ -by- $q$  tile matrix, we seek to find an appropriate sequence of unitary transformations on the tiled matrix so as to maximize parallelism (minimize critical path length). We will get our inspiration in previous work from the 70s/80s on Givens rotations where the question was somewhat related: given an  $m$ -by- $n$  matrix, find an appropriate sequence of Givens rotations as to maximize parallelism. This question is essentially answered in [6, 7, 12, 14]; we call this class of algorithms “coarse-grain algorithms.”

Working with tiles instead of scalars, we introduce four essential differences between the analysis and the reality of the tiled algorithms and the coarse-grain algorithms. First, while there are only two states for a scalar (nonzero or zero), a tile can be in three states (zero, triangle or full). Second, there are more operations available on tiles to introduce zeros; we have a total of three different tasks which can introduce zeros in a matrix. Third, the factorization and the update are dissociated to enable factorization stages to overlap with update stages. In the coarse-grain algorithm, the factorization and the associated update are considered as a single stage. Fourth and last, while coarse-grain algorithms have only one task, we end up with six different tasks, which have different computational weights; this dramatically complicates the critical path analysis of the tiled algorithms.

While the GREEDY algorithm is optimal for “coarse-grain algorithms”, we show that it is not in the case of tiled algorithms. We are unable to devise an optimal algorithm at this point, but we can prove that both GREEDY and FIBONACCI are asymptotically optimal for all matrices of size  $p = q^2 f(q)$ , where  $f$  is any function such that  $\lim_{+\infty} f = 0$ . This result applies to all matrices where  $p$  and  $q$  are proportional,  $p = \lambda q$ , with  $\lambda \geq 1$ , thereby encompassing many important situations in practice (least squares).

This paper is organized as follows. Section 2 reviews the numerical kernels needed to perform a tiled QR factorization, and introduces elimination lists, which enable us to formally define tiled algorithms. Section 3 presents the core algorithmic contributions of this paper. One major result is the asymptotic

optimality of two new tiled algorithms, FIBONACCI and GREEDY. Section 4 is devoted to numerical experiments on multicore platforms. For tall matrices ( $p \geq 2q$ ), these experiments confirm the superiority of the new algorithms over state-of-the-art solutions of the PLASMA library [4, 5, 8, 10]. Finally, we provide some concluding remarks in Section 5.

## 2 The QR factorization algorithm

Tiled algorithms are expressed in terms of tile operations rather than elementary operations. Each tile is of size  $n_b \times n_b$ , where  $n_b$  is a parameter tuned to squeeze the most out of arithmetic units and memory hierarchy. Typically,  $n_b$  ranges from 80 to 200 on state-of-the-art machines [2]. Algorithm 1 outlines a naive tiled QR algorithm, where loop indices represent tiles:

---

**Algorithm 1:** Naive QR algorithm for a tiled  $p \times q$  matrix.

---

```

for  $k = 1$  to  $\min(p, q)$  do
  for  $i = k + 1$  to  $p$  do
     $\lfloor$   $\text{elim}(i, \text{piv}(i, k), k)$ 

```

---

In Algorithm 1,  $k$  is the panel index, and  $\text{elim}(i, \text{piv}(i, k), k)$  is an orthogonal transformation that combines rows  $i$  and  $\text{piv}(i, k)$  to zero out the tile in position  $(i, k)$ . However, this formulation is somewhat misleading, as there is much more freedom for QR factorization algorithms than, say, for Cholesky algorithms (and contrarily to LU elimination algorithms, there are no numerical stability issues). For instance in column 1, the algorithm must eliminate all tiles  $(i, 1)$  where  $i > 1$ , but it can do so in several ways. Take  $p = 6$ . Algorithm 1 uses the transformations

$$\text{elim}(2, 1, 1), \text{elim}(3, 1, 1), \text{elim}(4, 1, 1), \text{elim}(5, 1, 1), \text{elim}(6, 1, 1)$$

But the following scheme is also valid:

$$\text{elim}(3, 1, 1), \text{elim}(6, 4, 1), \text{elim}(2, 1, 1), \text{elim}(5, 4, 1), \text{elim}(4, 1, 1)$$

In this latter scheme, the first two transformations  $\text{elim}(3, 1, 1)$  and  $\text{elim}(6, 4, 1)$  use distinct pairs of rows, and they can execute in parallel. On the contrary,  $\text{elim}(3, 1, 1)$  and  $\text{elim}(2, 1, 1)$  use the same pivot row and must be sequentialized. To complicate matters, it is possible to have two orthogonal transformations that execute in parallel but involve zeroing a tile in two different columns. For instance we can add  $\text{elim}(6, 5, 2)$  to the previous transformations and run it concurrently with, say,  $\text{elim}(2, 1, 1)$ . Any tiled QR algorithm will be characterized by an *elimination list*, which provides the ordered list of the transformations used to zero out all the tiles below the diagonal. This elimination list must obey certain conditions so that the factorization is valid. For instance,  $\text{elim}(6, 5, 2)$  must follow  $\text{elim}(6, 4, 1)$  and  $\text{elim}(5, 4, 1)$  in the previous list, because there is a flow dependence between these transformations. Note that, although the elimination list is given as a totally ordered sequence, some transformations can execute in parallel, provided that they are not linked by a dependence: in the



| Operation                          | Panel        |      | Update       |      |
|------------------------------------|--------------|------|--------------|------|
|                                    | Name         | Cost | Name         | Cost |
| Factor square into triangle        | <i>GEQRT</i> | 4    | <i>UNMQR</i> | 6    |
| Zero square with triangle on top   | <i>TSQRT</i> | 6    | <i>TSMQR</i> | 12   |
| Zero triangle with triangle on top | <i>TTQRT</i> | 2    | <i>TTMQR</i> | 6    |

Table 1: Kernels for tiled QR. The unit of time is  $\frac{n_b^3}{3}$ , where  $n_b$  is the blocksize.

example,  $elim(6, 4, 1)$  and  $elim(2, 1, 1)$  could have been swapped, and the elimination list would still be valid.

Before formally stating the conditions that guarantee the validity of (the elimination list of) an algorithm, we explain how orthogonal transformations can be implemented.

## 2.1 Kernels

To implement a given orthogonal transformation  $elim(i, piv(i, k), k)$ , one can use six different kernels, whose costs are given in Table 1. In this table, the unit of time is the time to perform  $\frac{n_b^3}{3}$  floating-point operations [3].

There are two main possibilities to implement an orthogonal transformation  $elim(i, piv(i, k), k)$ : The first version eliminates tile  $(i, k)$  with the *TS* (*Triangle on top of square*) kernels, as shown in Algorithm 2:

---

**Algorithm 2:** Elimination  $elim(i, piv(i, k), k)$  via *TS* (*Triangle on top of square*) kernels.

---

```

GEQRT(piv(i, k), k)
TSQRT(i, piv(i, k), k)
for j = k + 1 to q do
  UNMQR(piv(i, k), k, j)
  TSMQR(i, piv(i, k), k, j)

```

---

Here the tile panel  $(piv(i, k), k)$  is factored into a triangle (with *GEQRT*). The transformation is applied to subsequent tiles  $(piv(i, k), j)$ ,  $j > k$ , in row  $piv(i, k)$  (with *UNMQR*). Tile  $(i, k)$  is zeroed out (with *TSQRT*), and subsequent tiles  $(i, j)$ ,  $j > k$ , in row  $i$  are updated (with *TSMQR*). The flop count is  $4 + 6 + (6 + 12)(q - k) = 10 + 18(q - k)$  (expressed in same time unit as in Table 1). Dependencies are the following:

$$\begin{aligned}
&GEQRT(piv(i, k), k) \prec TSQRT(i, piv(i, k), k) \\
&GEQRT(piv(i, k), k) \prec UNMQR(piv(i, k), k, j) \quad \text{for } j > k \\
&UNMQR(piv(i, k), k, j) \prec TSMQR(i, piv(i, k), k, j) \quad \text{for } j > k \\
&TSQRT(i, piv(i, k), k) \prec TSMQR(i, piv(i, k), k, j) \quad \text{for } j > k
\end{aligned}$$

Note that  $TSQRT(i, piv(i, k), k)$  and  $UNMQR(piv(i, k), k, j)$  can be executed in parallel, as well as *UNMQR* operations on different columns  $j, j' > k$ . With an unbounded number of processors, the parallel time is thus  $4 + 6 + 12 = 22$  time-units.

The second approach to implement the orthogonal transformation  $\text{elim}(i, \text{piv}(i, k), k)$  is with the  $TT$  (*Triangle on top of triangle*) kernels, as shown in Algorithm 3:

---

**Algorithm 3:** Elimination  $\text{elim}(i, \text{piv}(i, k), k)$  via  $TT$  (*Triangle on top of triangle*) kernels.

---

```

GEQRT(piv(i, k), k)
GEQRT(i, k)
for j = k + 1 to q do
  UNMQR(piv(i, k), k, j)
  UNMQR(i, k, j)
TTQRT(i, piv(i, k), k)
for j = k + 1 to q do
  TTMQR(i, piv(i, k), k, j)

```

---

Here both tiles  $(\text{piv}(i, k), k)$  and  $(i, k)$  are factored into a triangle (with  $GEQRT$ ). The corresponding transformations are applied to subsequent tiles  $(\text{piv}(i, k), j)$  and  $(i, j)$ ,  $j > k$ , in both rows  $\text{piv}(i, k)$  and  $i$  (with  $UNMQR$ ). Tile  $(i, k)$  is zeroed out (with  $TTQRT$ ), and subsequent tiles  $(i, j)$ ,  $j > k$ , in row  $i$  are updated (with  $TTMQR$ ). The flop count is  $2(4 + 6(q - k)) + 2 + 6(q - k) = 10 + 18(q - k)$ , just as before. Dependencies are the following:

$$\begin{array}{ll}
GEQRT(\text{piv}(i, k), k) \prec UNMQR(\text{piv}(i, k), k, j) & \text{for } j > k \\
GEQRT(i, k) \prec UNMQR(i, k, j) & \text{for } j > k \\
GEQRT(\text{piv}(i, k), k) \prec TTQRT(i, \text{piv}(i, k), k) & \\
GEQRT(i, k) \prec TTQRT(i, \text{piv}(i, k), k) & \\
TTQRT(i, \text{piv}(i, k), k) \prec TTMQR(i, \text{piv}(i, k), k, j) & \text{for } j > k \\
UNMQR(\text{piv}(i, k), k, j) \prec TTMQR(i, \text{piv}(i, k), k, j) & \text{for } j > k \\
UNMQR(i, k, j) \prec TTMQR(i, \text{piv}(i, k), k, j) & \text{for } j > k
\end{array}$$

Now the factor operations in row  $\text{piv}(i, k)$  and  $i$  can be executed in parallel. Moreover, the  $UNMQR$  updates can be run in parallel with the  $TTQRT$  factorization. Thus, with an unbounded number of processors, the parallel time is  $4 + 6 + 6 = 16$  time-units.

All the new algorithms introduced in this paper are based on  $TT$  (kernels). From an algorithmic perspective,  $TT$  kernels are more appealing than  $TS$  kernels, as they offer more parallelism. More precisely, we can always break a  $TS$  kernel into two  $TT$  kernels: We can replace a  $TSQRT(i, \text{piv}(i, k), k)$  (following a  $GEQRT(\text{piv}(i, k), k)$ ) by a  $GEQRT(i, k)$  and a  $TTQRT(i, \text{piv}(i, k), k)$ . A similar transformation can be made for the updates. Hence a  $TS$ -based tiled algorithm can always be executed with  $TT$  kernels, while the converse is not true. However, the  $TS$  kernels provide more data locality, they benefit from a very efficient implementation (see Section 4), and several existing algorithms use these kernels. For all these reasons, and for comprehensiveness, our experiments will compare approaches based on both kernel types.

## 2.2 Elimination lists

As stated above, any algorithm factorizing a tiled matrix of size  $p \times q$  is characterized by its elimination list. Obviously, the algorithm must zero out all tiles below the diagonal: for each tile  $(i, k)$ ,  $i > k$ ,  $1 \leq k \leq \min(p, q)$ , the list must contain exactly one entry  $\text{elim}(i, \star, k)$ , where  $\star$  denotes some row index  $\text{piv}(i, k)$ . There are two conditions for a transformation  $\text{elim}(i, \text{piv}(i, k), k)$  to be valid:

- both rows  $i$  and  $\text{piv}(i, k)$  must be ready, meaning that all their tiles left of the panel (of indices  $(i, k')$  and  $(\text{piv}(i, k), k')$  for  $1 \leq k' < k$ ) must have already been zeroed out: all transformations  $\text{elim}(i, \text{piv}(i, k'), k')$  and  $\text{elim}(\text{piv}(i, k), \text{piv}(\text{piv}(i, k), k'), k')$  must precede  $\text{elim}(i, \text{piv}(i, k), k)$  in the elimination list
- row  $\text{piv}(i, k)$  must be a potential annihilator, meaning that tile  $(\text{piv}(i, k), k)$  has not been zeroed out yet:  
the transformation  $\text{elim}(\text{piv}(i, k), \text{piv}(\text{piv}(i, k), k), k)$  must follow  $\text{elim}(i, \text{piv}(i, k), k)$  in the elimination list

Any algorithm that factorizes the tiled matrix obeying these conditions is called a *generic tiled algorithm* in the following.

## 2.3 Execution schemes

In essence, the execution of a generic tiled algorithm is fully determined by its elimination list. This list is statically given as input to the scheduler, and the execution progresses dynamically, with the scheduler executing all required transformations as soon as possible. More precisely, each transformation involves several kernels, whose execution starts as soon as they are ready, i.e., as soon as all dependencies have been enforced. Recall that a tile  $(i, k)$  can be zeroed out only after all tiles  $(i, k')$ , with  $k' < k$ , have been zeroed out. Execution progresses as follows:

- Before being ready for elimination, tile  $(i, k)$ ,  $i > k$ , must be updated  $k - 1$  times, in order to zero out the  $k - 1$  tiles to its left (of index  $(i, k')$ ,  $k' < k$ ). The last update is a transformation  $\text{TTMQR}(i, \text{piv}(i, k - 1), k - 1, k)$  for some row index  $\text{piv}(i, k - 1)$  such that  $\text{elim}(i, \text{piv}(i, k - 1), k - 1)$  belongs to the elimination list. When completed, this transformation triggers the transformation  $\text{GEQRT}(i, k)$ , which can be executed immediately after the completion of the  $\text{TTMQR}$ . In turn,  $\text{GEQRT}(i, k)$  triggers all updates  $\text{UNMQR}(i, k, j)$  for all  $j > k$ . These updates are executed as soon as they are ready for execution.
- The elimination  $\text{elim}(i, \text{piv}(i, k), k)$  is performed as soon as possible when both rows  $i$  and  $\text{piv}(i, k)$  are ready. Just after the completion of  $\text{GEQRT}(i, k)$  and  $\text{GEQRT}(\text{piv}(i, k), k)$ , kernel  $\text{TTQRT}(i, \text{piv}(i, k), k)$  is launched. When finished, it triggers the updates  $\text{TTMQR}(i, \text{piv}(i, k), k, j)$  for all  $j > k$ .

Obviously, the degree of parallelism that can be achieved depends upon the eliminations that are chosen. For instance, if all eliminations in a given column use the same factor tile, they will be sequentialized. This corresponds to the flat tree elimination scheme described below: in each column  $k$ , it uses  $\text{elim}(i, k, k)$  for all  $i > k$ . On the contrary, two eliminations  $\text{elim}(i, \text{piv}(i, k), k)$

and  $\text{elim}(i', \text{piv}(i', k), k)$  in the same column can be fully parallelized provided that they involve four different rows. Finally, note that several eliminations can be initiated in different columns simultaneously, provided that they involve different pairs of rows, and that all these rows are ready (i.e., they have the desired number of leftmost zeros).

The following lemma will prove very useful; it states that we can assume w.l.o.g. that each tile is zeroed out by a tile above it, closer to the diagonal.

**Lemma 1.** *Any generic tiled algorithm can be modified, without changing its execution time, so that all eliminations  $\text{elim}(i, \text{piv}(i, k), k)$  satisfy to  $i > \text{piv}(i, k)$ .*

*Proof.* Define a *reverse* elimination as an elimination  $\text{elim}(i, \text{piv}(i, k), k)$  where  $i < \text{piv}(i, k)$ . Consider a generic tiled algorithm whose elimination list contains some reverse eliminations. Let  $k_0$  be the first column to contain one of them. Let  $i_0$  be the largest row index involved in a reverse elimination in column  $k_0$ . The elimination list in column  $k_0$  may contain several reverse eliminations  $\text{elim}(i_1, i_0, k_0)$ ,  $\text{elim}(i_2, i_0, k_0)$ ,  $\dots$ ,  $\text{elim}(i_r, i_0, k_0)$ , in that order, before row  $i_0$  is eventually zeroed out by the transformation  $\text{elim}(i_0, \text{piv}(i_0, k_0), k_0)$ . Note that  $\text{piv}(i_0, k_0) < i_0$  by definition of  $i_0$ . We modify the algorithm by exchanging the roles of rows  $i_0$  and  $i_1$  in column  $k_0$ : the elimination list now includes  $\text{elim}(i_0, i_1, k_0)$ ,  $\text{elim}(i_2, i_1, k_0)$ ,  $\dots$ ,  $\text{elim}(i_r, i_1, k_0)$ , and  $\text{elim}(i_1, \text{piv}(i_0, k_0), k_0)$ . All dependencies are preserved, and the execution time is unchanged. Now the largest row index involved in a reverse elimination in column  $k_0$  is strictly smaller than  $i_0$ , and we repeat the procedure until there does not remain any reverse elimination in column  $k_0$ . We proceed inductively to the following columns, until all reverse eliminations have been suppressed.  $\square$

### 3 Critical paths

In this section we describe several generic tiled algorithms, and we provide their critical paths, as well as optimality results. These algorithms are inspired by algorithms that have been introduced twenty to thirty years ago [14, 12, 7, 6], albeit for a much simpler, *coarse-grain* model. In this “old” model, the time-unit is the time needed to execute an orthogonal transformation across two matrix rows, regardless of the position of the zero to be created, hence regardless of the length of these rows. Although the granularity is much coarser in this model, any existing algorithm for the old model can be transformed into a generic tiled algorithm, just by enforcing the very same elimination list provided by the algorithm. Critical paths are obtained using a discrete event based simulator specially developed to this end, based on the Simgrid framework [15]. It carefully handles dependencies across tiles, and allows for the analysis of both static and dynamic algorithms.<sup>1</sup>

#### 3.1 Coarse-grain algorithms

We start with a short description of three algorithms for the coarse-grain model. These algorithms are illustrated in Table 2 for a  $15 \times 6$  matrix.

<sup>1</sup>The discrete event based simulator, together with the code for all tiled algorithms, is publicly available at <http://graal.ens-lyon.fr/~mjacquel/tiledQR.html>

**Sameh-Kuck algorithm** The SAMEH-KUCK algorithm [14] uses the panel row for all eliminations in each column, starting from below the diagonal and proceeding downwards. Time-steps indicate the time-unit at which the elimination can be done, assuming unbounded resources. Formally, the elimination list is

$$\left\{ \left( \text{elim}(i, k, k), i = k + 1, k + 2, \dots, p \right), k = 1, 2, \dots, \min(p, q) \right\}$$

**Fibonacci algorithm** The FIBONACCI algorithm is the Fibonacci scheme of order 1 in [12]. Let  $\text{coarse}(i, k)$  be the time-step at which tile  $(i, k)$ ,  $i > k$ , is zeroed out. These values are computed as follows. In the first column, there are one 5, two 4's, three 3's, four 2's and four 1's (we would have had five 1's with  $p = 16$ ). Given  $x$  as the least integer such that  $x(x + 1)/2 \geq p - 1$ , we have  $\text{coarse}(i, 1) = x - y + 1$  where  $y$  is the least integer such that  $i \leq y(y + 1)/2 + 1$ . Let the row indices of the  $z$  tiles that are zeroed out at step  $s$ ,  $1 \leq s \leq x$ , range from  $i$  to  $i + z - 1$ . The elimination list for these tiles is  $\text{elim}(i + j, \text{piv}(i + j, 1), 1)$ , with  $\text{piv}(i + j) = i + j - z$  for  $0 \leq j \leq z - 1$ . In other words, to eliminate a bunch of  $z$  consecutive tiles at the same time-step, the algorithm uses the  $z$  rows above them, pairing them in the natural order. Now the elimination scheme of the next column is the same as that of the previous column, shifted down by one row, and adding two time-units:  $\text{coarse}(i, k) = \text{coarse}(i - 1, k - 1) + 2$ , while the pairing obeys the same rule.

**Greedy algorithm** At each step, the GREEDY algorithm [7, 6] eliminates as many tiles as possible in each column, starting with bottom rows. The pairing for the eliminations is done exactly as for FIBONACCI. There is no closed-form formula to compute  $\text{coarse}(i, k)$ , the time-step at which tile  $(i, k)$  is eliminated, but it is possible to provide recursive expressions (see [7, 6]).

| (a) SAMEH-KUCK    | (b) FIBONACCI  | (c) GREEDY    |
|-------------------|----------------|---------------|
| *                 | *              | *             |
| 1 *               | 5 *            | 4 *           |
| 2 3 *             | 4 7 *          | 3 6 *         |
| 3 4 5 *           | 4 6 9 *        | 3 5 8 *       |
| 4 5 6 7 *         | 3 6 8 11 *     | 2 5 7 10 *    |
| 5 6 7 8 9 *       | 3 5 8 10 13 *  | 2 4 7 9 12 *  |
| 6 7 8 9 10 11     | 3 5 7 10 12 15 | 2 4 6 9 11 14 |
| 7 8 9 10 11 12    | 2 5 7 9 12 14  | 2 4 6 8 10 13 |
| 8 9 10 11 12 13   | 2 4 7 9 11 14  | 1 3 5 8 10 12 |
| 9 10 11 12 13 14  | 2 4 6 9 11 13  | 1 3 5 7 9 11  |
| 10 11 12 13 14 15 | 2 4 6 8 11 13  | 1 3 5 7 9 11  |
| 11 12 13 14 15 16 | 1 4 6 8 10 13  | 1 3 4 6 8 10  |
| 12 13 14 15 16 17 | 1 3 6 8 10 12  | 1 2 4 6 8 10  |
| 13 14 15 16 17 18 | 1 3 5 8 10 12  | 1 2 4 5 7 9   |
| 14 15 16 17 18 19 | 1 3 5 7 10 12  | 1 2 3 5 6 8   |

Table 2: Time-steps for coarse-grain algorithms.

Consider a rectangular  $p \times q$  matrix, with  $p > q$ . With the coarse-grain model, the critical path of SAMEH-KUCK is  $p + q - 2$ , and that of FIBONACCI is  $x + 2q - 2$ , where  $x$  is the least integer such that  $x(x + 1)/2 \geq p - 1$ . The critical path of GREEDY is unknown, but two important results are known: (i) the critical path of GREEDY is optimal; (ii) its value tends to  $2q$  if  $p$  is negligible in front of  $q^2$ , i.e., if we have  $p = q^2 f(q)$  where  $f$  is any function such that  $\lim_{+\infty} f = 0$  (and  $f(q) > 1/q$  so that  $p > q$ ). In particular, let  $p$  and  $q$  be proportional,  $p = \lambda q$ , with a constant  $\lambda > 1$ : FIBONACCI is asymptotically optimal, because  $x$  is of the order of  $\sqrt{\lambda q}$ , hence its critical path is  $2q + o(q)$ . On

the contrary, SAMEH-KUCK is not asymptotically optimal since its critical path is  $(1 + \lambda)q - 2$ . For square  $q \times q$  matrices, critical paths are slightly different ( $2q - 3$  for SAMEH-KUCK,  $x + 2q - 4$  for FIBONACCI), but the important result is that all three algorithms are asymptotically optimal in that case.

---

**Algorithm 4:** GREEDY algorithm via  $TT$  kernels.

---

```

for j = 1 to q do
  /* nz(j) is the number of tiles which have been eliminated in column j */
  nZ(j) = 0
  /* nT(j) is the number of tiles which have been triangularized in column j */
  nT(j) = 0
while column q is not finished do
  for j = q down to 1 do
    if j == 1 then
      /* Triangularize the first column if not yet done */
      nTnew = nT(j) + (p - nT(j))
      if p - nT(j) > 0 then
        for k = p down to 1 do
          GEQRT(k, j)
          for jj = j + 1 to q do
            UNMQR(k, j, jj)
        else
          /* Triangularize every tile having a zero in the previous column */
          nTnew = nZ(j - 1)
          for k = nT(j) to nTnew - 1 do
            GEQRT(p - k, j)
            for jj = j + 1 to q do
              UNMQR(p - k, j, jj)
          /* Eliminate every tile triangularized in the previous step */
          nZnew = nZ(j) + ⌊  $\frac{nT(j) - nZ(j)}{2}$  ⌋
          for kk = nZ(j) to nZnew - 1 do
            piv(p - kk) = p - kk - nZnew + nZ(j)
            TTQRT(p - kk, piv(p - kk), j)
            for jj = j + 1 to q do
              TTMQR(p - kk, piv(p - kk), j, jj)
          /* Update the number of triangularized and eliminated tiles at the next step */
          nT(j) = nTnew
          nZ(j) = nZnew

```

---

### 3.2 Tiled algorithms

As stated above, each coarse-grain algorithm can be transformed into a tiled algorithm, simply by keeping the same elimination list, and triggering the execution of each kernel as soon as possible. However, because the weights of the

| (a) SAMEH-KUCK           | (b) FIBONACCI         | (c) GREEDY           | (d) BINARY TREE       | (e) PLASMA TREE (BS = 5) |
|--------------------------|-----------------------|----------------------|-----------------------|--------------------------|
| 6 *                      | 14 *                  | 12 *                 | 6 *                   | 6 *                      |
| 8 28 *                   | 12 48 *               | 10 42 *              | 8 28 *                | 8 28 *                   |
| 10 34 50 *               | 12 46 70 *            | 10 40 64 *           | 6 36 56 *             | 10 34 50 *               |
| 12 40 56 72 *            | 10 42 68 92 *         | 8 36 62 86 *         | 10 34 70 90 *         | 12 40 56 72 *            |
| 14 46 62 78 94 *         | 10 40 64 90 114 *     | 8 34 56 84 106 *     | 6 44 68 104 124 *     | 14 46 62 78 94 *         |
| 16 52 68 84 100 116 *    | 10 40 62 86 112 136 * | 8 34 56 78 102 128 * | 8 28 78 102 138 158 * | 6 54 74 90 106 122 *     |
| 18 58 74 90 106 122 *    | 8 36 62 84 108 134 *  | 8 30 52 78 100 122 * | 6 42 62 112 136 172 * | 8 28 82 102 118 134 *    |
| 20 64 80 96 112 128 *    | 8 34 58 84 106 130 *  | 6 28 50 72 100 118 * | 12 40 76 96 146 170 * | 10 34 50 110 130 146 *   |
| 22 70 86 102 118 134 *   | 8 34 56 80 106 128 *  | 6 28 50 72 94 116 *  | 6 46 74 110 130 180 * | 12 40 56 72 138 158 *    |
| 24 76 92 108 124 140 *   | 8 34 56 78 102 128 *  | 6 28 50 68 94 116 *  | 8 28 80 108 144 164 * | 16 52 68 84 100 166 *    |
| 26 82 98 114 130 146 *   | 6 28 56 78 100 122 *  | 6 28 44 66 88 110 *  | 6 36 56 114 142 178 * | 6 56 80 96 112 128 *     |
| 28 88 104 120 136 152 *  | 6 28 50 78 100 122 *  | 6 22 44 66 88 110 *  | 10 34 64 84 148 176 * | 8 28 84 108 124 140 *    |
| 30 94 110 126 142 158 *  | 6 28 44 72 100 122 *  | 6 22 44 60 82 104 *  | 6 38 62 92 112 182 *  | 10 34 50 112 136 152 *   |
| 32 100 116 132 148 164 * | 6 22 44 60 94 116 *   | 6 22 38 60 76 98 *   | 8 28 66 90 114 134 *  | 12 40 56 72 140 164 *    |

Table 3: Time-steps for tiled algorithms.

factor and update kernels are not the same, it is much more difficult to compute the critical paths of the transformed (tiled) algorithms. Table 3 is the counterpart of Table 2, and depicts the time-steps at which tiles are actually zeroed out. Note that the tiled version of SAMEH-KUCK is indeed the FLATTREE algorithm in PLASMA [4, 5], and we have renamed it accordingly. As an example, Algorithm 4 shows the GREEDY algorithm for the tiled model.

A first (and quite unexpected) result is that GREEDY is no longer optimal, as shown in the first two columns of Table 4a for a  $15 \times 2$  matrix. In each column and at each step, the **ASAP algorithm** starts the elimination of a tile as soon as there are at least two rows ready for the transformation. When  $s \geq 2$  eliminations can start simultaneously, ASAP pairs the  $2s$  rows just as FIBONACCI and GREEDY, the first row (closest to the diagonal) with row  $s + 1$ , the second row with row  $s + 2$ , and so on. As a matter of fact, when processing the second column, both ASAP and GREEDY begin with the elimination of lines 10 to 15 (at time step 20). However, once tiles (13, 2), (14, 2) and (15, 2) are zeroed out (i.e. at time step 22), ASAP eliminates 4 zeros, in rows 9 through 12. On the contrary, GREEDY waits until time step 26 to eliminate 6 zeros in rows 6 through 12. In a sense, ASAP is the counterpart of GREEDY at the tile level. However, ASAP is not optimal either, as shown in Table 4a for a  $15 \times 3$  matrix. On larger examples, the critical path of GREEDY is better than that of ASAP, as shown in Table 4b.

(a) GREEDY nor ASAP are optimal.

| (a) GREEDY |    |    | (b) ASAP |    |    |
|------------|----|----|----------|----|----|
| *          |    |    | *        |    |    |
| 12         | *  |    | 12       | *  |    |
| 10         | 42 | *  | 10       | 40 | *  |
| 10         | 40 | 64 | 10       | 36 | 86 |
| 8          | 36 | 62 | 8        | 34 | 80 |
| 8          | 34 | 56 | 8        | 32 | 74 |
| 8          | 34 | 56 | 8        | 30 | 68 |
| 8          | 30 | 52 | 8        | 28 | 62 |
| 6          | 28 | 50 | 6        | 28 | 56 |
| 6          | 28 | 50 | 6        | 26 | 50 |
| 6          | 28 | 50 | 6        | 24 | 46 |
| 6          | 28 | 44 | 6        | 24 | 44 |
| 6          | 22 | 44 | 6        | 22 | 44 |
| 6          | 22 | 44 | 6        | 22 | 40 |
| 6          | 22 | 38 | 6        | 22 | 38 |

(b) GREEDY generally outperforms ASAP.

| $p$ | Algorithm | $q$ |      |      |      |
|-----|-----------|-----|------|------|------|
|     |           | 16  | 32   | 64   | 128  |
| 16  | GREEDY    | 310 |      |      |      |
|     | ASAP      | 310 |      |      |      |
| 32  | GREEDY    | 360 | 650  |      |      |
|     | ASAP      | 402 | 656  |      |      |
| 64  | GREEDY    | 374 | 726  | 1342 |      |
|     | ASAP      | 588 | 844  | 1354 |      |
| 128 | GREEDY    | 396 | 748  | 1452 | 2732 |
|     | ASAP      | 966 | 1222 | 1748 | 2756 |

Table 4: Neither GREEDY nor ASAP are optimal.

We have a closed-form formula for the critical path of tiled FLATTREE, but not for that of tiled FIBONACCI (contrarily to the coarse-grain case). But we provide an asymptotic expression, both for FIBONACCI and for GREEDY. More importantly, we show that both tiled algorithms are asymptotically optimal. We state our main result:

**Theorem 1.** For a tiled matrix of size  $p \times q$ , where  $p \geq q$ :

1. The critical path length of FLATTREE is  $2p + 2$  if  $p \geq q = 1$ ,  $6p + 16q - 22$  if  $p > q > 1$  and  $22q - 24$  if  $p = q > 1$

2. The critical path length of FIBONACCI is at most  $22q + 6\lceil\sqrt{2p}\rceil$ , and that of GREEDY is at most  $22q + 6\lceil\log_2 p\rceil$
3. The optimal critical path length is at least  $22q - 30$
4. FIBONACCI is asymptotically optimal if  $p = q^2 f(q)$ , where  $\lim_{+\infty} f = 0$
5. GREEDY is asymptotically optimal if  $\log_2 p = qf(q)$ , where  $\lim_{+\infty} f = 0$

*Proof. Proof of (1).* Consider first the case  $p \geq q = 1$ . We shall proceed by induction on  $p$  to show that the critical path of FLATTREE is of length  $2p + 2$ . If  $p = 1$ , then from Table 1 the result is obtained since only  $GEQRT(1, 1)$  is required. With the base case established, now assume that this holds for all  $p-1 > q = 1$ . Thus at time  $t = 2(p-1)+2 = 2p$ , we have that for all  $p-1 \geq i \geq 1$  tile  $(i, 1)$  has been factorized into a triangle and for all  $p-1 \geq i > 1$ , tile  $(i, 1)$  has been zeroed out. Therefore, tile  $(p, 1)$  will be zeroed out with  $TTQRT(p, 1)$  at time  $t + 2 = 2(p-1) + 2 + 2 = 2p + 2$ .

Consider now the case  $p > q > 1$ . We show by induction on  $k$  that tile  $(i, k)$ , for  $i > k \geq 2$ , is zeroed out in FLATTREE at time unit  $6i + 16k - 22$ . For  $k = 2$ , tile  $(2, 2)$  is updated from step  $k = 1$  at time  $4 + 6 + 6 = 16$ , and it is factored into a triangle at time 20. Tile  $(3, 2)$  is updated from step  $k = 1$  at time 22 factored into a triangle at time 26 and then zeroed out at time  $26 + 2 = 28 = 6 \times 3 + 16 \times 2 - 22$ . A new tile in column 2 is zeroed out every 6 time units, hence the initialization of the induction for  $k = 2$ . Assume now that the formula holds up to column  $k$ , and let  $t = 6(k+1) + 16k - 22$  be the time at which tile  $(k+1, k)$  is zeroed out. Tile  $(k+1, k+1)$  is updated from step  $k$  at time  $t - 2 + 6 + 6 = t + 10$  and factored into a triangle at time  $t + 14$ . By induction, tile  $(k+2, k)$  is zeroed out at time  $t + 6$ , hence triangularized at time  $t + 4$ . The corresponding  $UNMQR$  update of tile  $(k+2, k+1)$  ends at time  $t + 10$ , its  $TTMQR$  update ends at time  $\max(t + 14, t + 10) + 6 = t + 20$ . Hence tile  $(k+2, k+1)$  can indeed be zeroed out at time  $\max(t + 12, t + 20) + 2 = t + 22$ . A new tile in column  $k+1$  can be zeroed out every 6 time units, hence the induction formula for  $k+1$ .

Finally, for a square matrix of size  $q \times q$ , consider the above formula for a rectangular matrix with  $p = q + 1$ . Instead of zeroing out the last tile  $(q+1, q)$  with tile  $(q, q)$ , simply need to factor tile  $(q, q)$  into a triangle with  $GEQRT(q, q)$ . This costs 4 time units instead of 6 when adding  $TTQRT(q+1, q, q)$ , and explains the difference of 2 in the formula for square matrices.

**Proof of (2).** FIBONACCI and GREEDY are more difficult to analyze than FLATTREE, but we provide an upper bound of their critical path. The approach is the same for both algorithms, and hereafter ALG denotes either FIBONACCI or GREEDY. Let  $coarse(i, k)$  be the time-step at which tile  $(i, k)$  is zeroed out in ALG with the coarse-grain model (see Table 2 for examples). We derive a “slowed down” version of the tiled version of ALG by terminating the zeroing out of tile  $(i, k)$  at time-step

$$6coarse(2, 1) + 22(k-1) - 6(coarse(k, k) - coarse(i, k)).$$

We say that this version is slowed down because we do not start the zeroing out of the tiles as soon as possible. For instance in the first column, tile  $(i, 1)$  is zeroed out at time  $6coarse(i, k)$ , which is larger than the value given in Table 3. However, we keep the same elimination list as in the original version of ALG, and we trigger the update and factor operations as soon as possible when the zeroing out operation is completed. We only delay these latter operations.



The intuitive idea for delaying the eliminations is that the corresponding updates will be fully overlapped, within a given column, or when proceeding from one column to the next: in this case, allowing for a time-shift of 22 smooths the chaining of the updates. The regular and repetitive spacing of the eliminations allows us to check (just as we did to prove (1)) that all dependencies are enforced in the slowed down version of ALG. Because the case-analysis is tedious, we have written a program for a sanity check of the validity of ALG<sup>2</sup>.

In the coarse-grain model, ALG terminates the first column in time  $x$ , so the critical path of its slowed down version is  $6x + 22(q - 1)$ . For FIBONACCI,  $x$  is the least integer such that  $x(x + 1)/2 \geq p - 1$ , hence  $x \leq \lceil \sqrt{2p} \rceil$ . For GREEDY,  $x = \lceil \log_2(p - 1) \rceil \leq \lceil \log_2 p \rceil$ , hence the result.

**Proof of (3).** Consider a square  $q \times q$  matrix  $B$ , with  $q \geq 2$ . Assume that there are only three non-zero sub-diagonals, i.e., that tile  $(i, k)$  is initially zero in  $B$  for  $i > k + 3$ . Because there are only three non-zero tiles below the diagonal, there is a constant number of possible row pairings in each column. An exhaustive search is to try all possible pairings in the first column, followed by all possible pairings in the second column, and so on. After a few columns, a pattern emerges, and we can identify that any optimal algorithm (there are several of them) needs at least 22 time-steps to proceed from one column to the next. It is possible to save a few steps at the beginning and end of the execution, and the optimal critical path is  $22q - 30$ . Here also, because the case-analysis is long and tedious, we have written a program for a sanity check of the latter value.

Now we show that the optimal critical path for a general  $p \times q$  matrix  $A$ , with  $p \geq q \geq 2$ , is at least equal to the critical path of the previous  $q \times q$  matrix  $B$  with three sub-diagonals. Indeed, Lemma 1 shows that there exist optimal algorithms for factoring  $A$  without any reverse elimination. Consider such an algorithm, and discard all eliminations that involve zeroing out elements below the third sub-diagonal, or outside the  $q \times q$  top square: the critical path cannot increase, and we have an elimination scheme for  $B$ , which proves the desired result.

Note that using  $B$  instead of  $A$  is the key to the proof: in each column of  $B$ , there is only a constant number of possible row pairings, which makes it possible to try all combinations for several consecutive columns. Reasoning with  $A$  instead would need a completely different proof (yet to be invented).

**Proof of (4) and (5).** These are a direct consequence of (3) and (4).  $\square$

In Table 3 we also report time-steps for the BINARYTREE algorithm in PLASMA [8]. As its name indicates, this algorithm performs a binary tree reduction to zero out tiles in each column. Here is an asymptotic expression of its critical path:

**Proposition 1.** *Consider a tiled matrix of size  $p \times q$ , where  $p \geq q$ . The critical path length of BINARYTREE is  $6q \log_2 p + o(q \log_2 p)$ .*

*Proof.* It is possible to derive an exact expression for the critical path length of BINARYTREE in the special case where  $p$  and  $q$  are both exact powers of two, with  $q < p$ . We obtain the value  $(10 + 6 \log_2 p)q - 4 \log_2 p - 6$ . As before, the

<sup>2</sup>All program sources are publicly available at <http://graal.ens-lyon.fr/~mjacquel/tiledQR.html>

proof goes by (tedious) induction. Here again, we have written a program for a sanity check of the latter value. The asymptotic value follows easily for an arbitrary matrix, by enlarging each dimension to the nearest power of two.  $\square$

Proposition 1 shows that BINARYTREE is not asymptotically optimal, but performs best for tall and skinny matrices. The PLASMA library provides more algorithms, that can be informally described as trade-offs between FLATTREE and BINARYTREE. These algorithms are referred to as PLASMATREE in all the following, and differ by the value of an input parameter called the *domain size*  $BS$ . This domain size can be any value between 1 and  $p$ , inclusive. Within a domain, that includes  $BS$  consecutive rows, the algorithm works just as FLATTREE: the first row of each domain acts as a local panel and is used to zero out the tiles in all the other rows of the domain. Then the domains are merged: the panel rows are zeroed out by a binary tree reduction, just as in BINARYTREE. As the algorithm progresses through the columns, the domain on the very bottom is reduced accordingly, until such time that there is one less domain. For the case that  $BS = 1$ , PLASMATREE follows a binary tree on the entire column, and for  $BS = p$ , the algorithm executes a flat tree on the entire column. It seems very difficult for a user to select the domain size  $BS$  leading to best performance, but it is known that  $BS$  should increase as  $q$  increases. Table 3 shows the time-steps of PLASMATREE with a domain size of  $BS = 5$ . In the experiments of Section 4, we use all possible values of  $BS$  and retain the one leading to the best value.

## 4 Experimental results

All experiments were performed on a 48-core machine composed of eight hexa-core AMD Opteron 8439 SE (codename Istanbul) processors running at 2.8 GHz. Each core has a theoretical peak of 11.2 Gflop/s with a peak of 537.6 Gflop/s for the whole machine. The Istanbul micro-architecture is a NUMA architecture where each socket has 6 MB of level-3 cache and each processor has a 512 KB level-2 cache and a 128 KB level-1 cache. After having benchmarked the AMD ACML and Intel MKL BLAS libraries, we selected MKL (10.2) since it appeared to be slightly faster in our experimental context. Linux 2.6.32 and Intel Compilers 11.1 were also used in conjunction with PLASMA 2.3.1.

For all results, we show both double and double complex precision, using all 48 cores of the machine. The matrices are of size  $m = 8000$  and  $200 \leq n \leq 8000$ . The tile size is kept constant at  $n_b = 200$ , so that the matrices can also be viewed as  $p \times q$  tiled matrices where  $p = 40$  and  $1 \leq q \leq 40$ . All kernels use an inner blocking parameter of  $i_b = 32$ .

The PLASMA interface allows one to specify the dependencies between tasks by designating the data as either INPUT, OUTPUT, INOUT, or NODEP. In our experimental context, we found that the update kernels (*UNMQR*, *TTMQR*, and *TSMQR*) introduced false dependencies between the tasks which sequentializes the execution of update with the factorization kernels *TTQRT* or *TSQRT*. In order to alleviate these, we altered the dependency designation within each of the update kernels for the matrix of Householder reflectors,  $V$ , from INPUT to NODEP as is further explained in [11]. The dependencies between the tasks are still consistent since the  $T$  matrix within each update kernel continues to

be designated as INPUT so that any subsequent task which overwrites this T matrix cannot be executed.

For each experiment, we provide a comparison of the theoretical performance to the actual performance. The theoretical performance is obtained by modeling the limiting factor of the execution time as either the critical path, or the sequential time divided by the number of processors. This is similar in approach to the Roofline model [17]. Taking  $\gamma_{seq}$  as the sequential performance,  $T$  as the total number of flops,  $cp$  as the length of the critical path, and  $P$  as the number of processors, the predicted performance,  $\gamma_{pred}$ , is

$$\gamma_{pred} = \frac{\gamma_{seq} \cdot T}{\max\left(\frac{T}{P}, cp\right)}$$

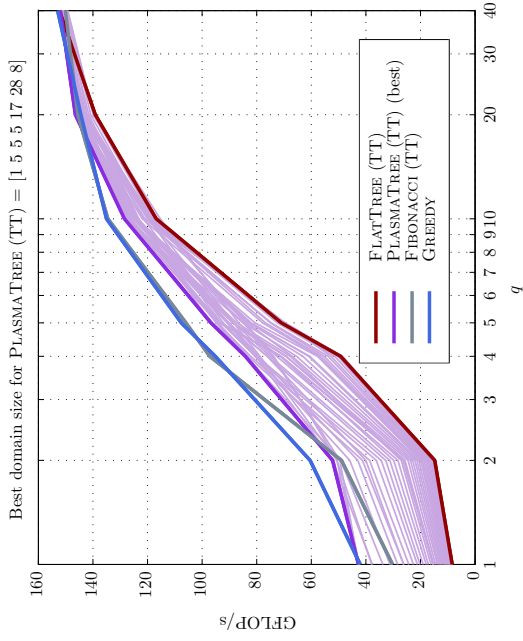
Figures 1a and 1c depict the predicted performance of all algorithms which use the *Triangle on top of triangle* kernels. For double complex precision, sequential kernels reach 3.1860 GFlop/s while in double precision, the peak performance is 3.8440 GFlop/s. Since PLASMATREE provides an additional tuning parameter of the domain size, we show the results for each value of this parameter as well as the composition of the best of these domain sizes. Again, it is not evident what the domain size should be for the best performance, hence our exhaustive search.

Part of our comprehensive study also involved comparisons made to the Semi-Parallel Tile and Fully-Parallel Tile CAQR algorithms found in [9] which are much the same as those found in PLASMA. As with PLASMA, the tuning parameter  $BS$  controls the domain size upon which a flat tree is used to zero out tiles below the root tile within the domain and a binary tree is used to merge these domains. Unlike PLASMA, it is not the bottom domain whose size decreases as the algorithm progresses through the columns, but instead is the top domain. In this study, we found that the PLASMA algorithms performed identically or better than these algorithms and therefore we do not report these comparisons.

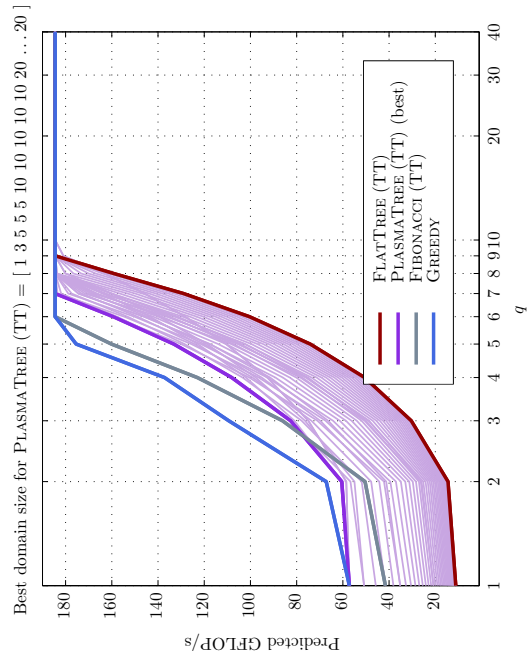
Figure 1b and 1d illustrate the experimental performance reached by GREEDY, FIBONACCI and PLASMATREE algorithms using the *TT (Triangle on top of triangle)* kernels. In both cases, double or double complex precision, the performance of GREEDY is better than PLASMATREE even for the best choice of domain size. Moreover, as expected from the analysis in Section 3.2, GREEDY outperforms FIBONACCI the majority of the time. Furthermore, we see that, for rectangular matrices, the experimental performance in double complex precision matches the prediction. This is not the case for double precision because communications have higher impact on performance.

While it is apparent that GREEDY does achieve higher levels of performance, the percentage may not be as obvious. To that end, taking GREEDY as the baseline, we present in Figure 2 the theoretical, double, and double complex precision overhead for each algorithm that uses the *Triangle on top of triangle* kernel as compared to GREEDY. These overheads are respectively computed in terms of critical path length and time. At a smaller scale (Figure 3), it can be seen that GREEDY can perform up to 13.6% better than PLASMATREE.

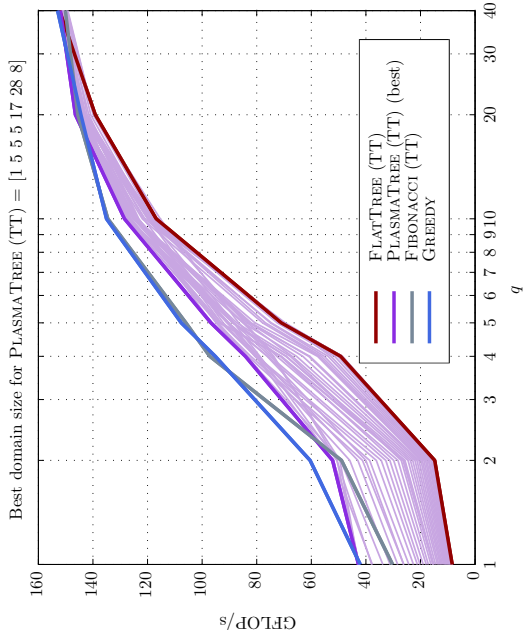
For all matrix sizes considered,  $p = 40$  and  $1 \leq q \leq 40$ , in the theoretical model, the critical path length for GREEDY is either the same as that of PLASMATREE ( $q = 1$ ) or is up to 25% shorter than PLASMATREE ( $q = 6$ ).



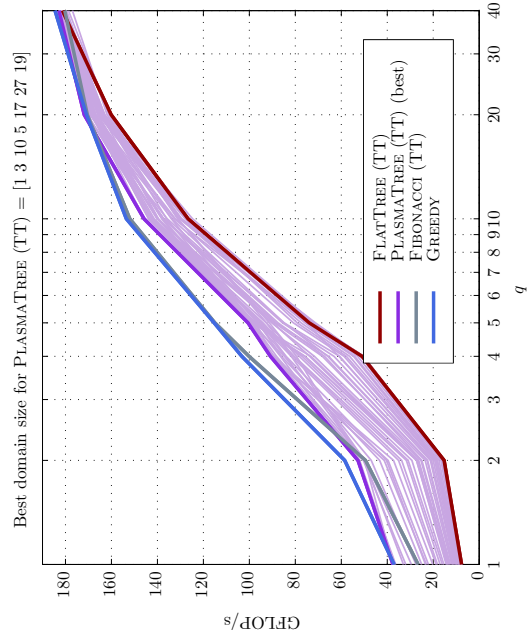
(a) Predicted (double complex)



(c) Predicted (double)

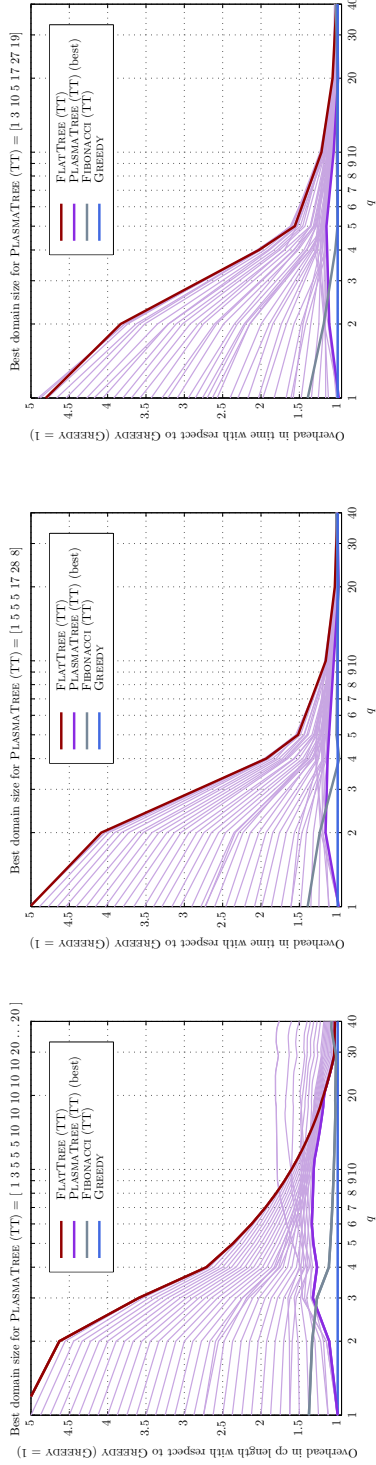


(b) Experimental (double complex)



(d) Experimental (double)

Figure 1: Predicted and experimental performance of QR factorization - Triangle on top of triangle kernels

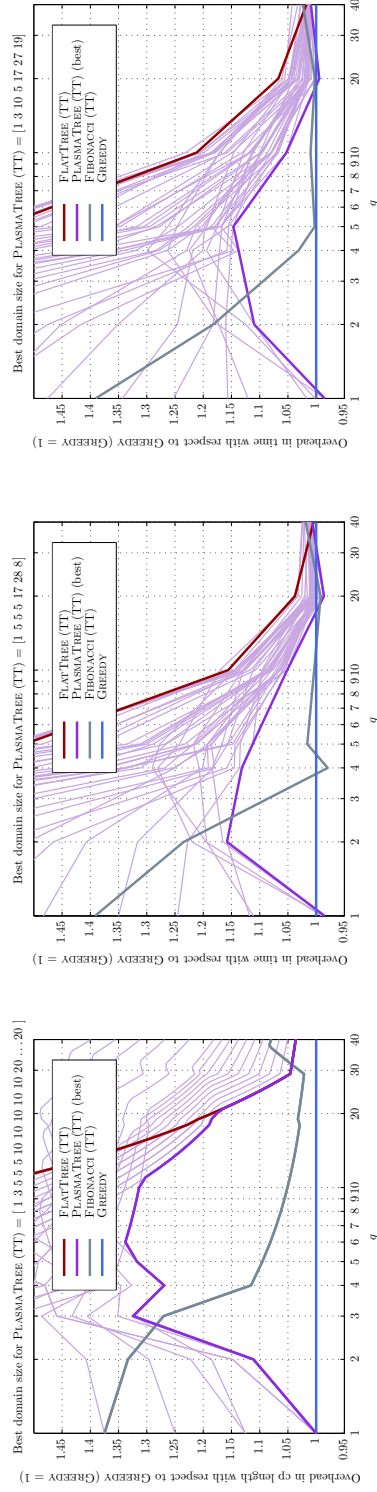


(a) Theoretical CP length

(b) Experimental (double complex)

(c) Experimental (double)

Figure 2: Overhead in terms of critical path length and time with respect to GREEDY (GREEDY = 1)



(a) Theoretical CP length

(b) Experimental (double complex)

(c) Experimental (double)

Figure 3: Detailed view of the overhead in terms of critical path length and time with respect to GREEDY (GREEDY = 1)

Analogously, the critical path length for GREEDY is at least 2% to 27% shorter than that of FIBONACCI. In the experiments, the matrix sizes considered were  $p = 40$  and  $q \in \{1, 2, 4, 5, 10, 20, 40\}$ . In double precision, GREEDY has a decrease of at most 1.5% than the best PLASMATREE ( $q = 1$ ) and a gain of at most 12.8% than the best PLASMATREE ( $q = 5$ ). In double complex precision, GREEDY has a decrease of at most 1.5% than the best PLASMATREE ( $q = 1$ ) and a gain of at most 13.6% than the best PLASMATREE ( $q = 2$ ). Similarly, in double precision, GREEDY provides a gain of 2.6% to 28.1% over FIBONACCI and in double complex precision, GREEDY has a decrease of at most 2.1% and a gain of at most 28.2% over FIBONACCI.

Although it is evidenced that PLASMATREE does not vary too far from GREEDY or FIBONACCI, one must keep in mind that there is a tuning parameter involved and we choose the best of these domain sizes for PLASMATREE to create the composite result, whereas with GREEDY, there is no such parameter to consider. Of particular interest is the fact that GREEDY always performs better than any other algorithm<sup>3</sup> for  $p \gg q$ . In the scope of PLASMATREE, a domain size  $BS = 1$  will force the use of a binary tree so that both GREEDY and PLASMATREE behave the same. However, as the matrix tends more to a square, i.e.,  $q$  tends toward  $p$ , we observe that the performance of all of the algorithms, including FLATTREE, are on par with GREEDY. As more columns are added, the parallelism of the algorithm is increased and the critical path becomes less of a limiting factor, so that the performance of the kernels is brought to the forefront. Therefore, all of the algorithms are performing similarly since they all share the same kernels.

In order to accurately assess the impact of the kernel selection towards the performance of the algorithms, Figures 4 and 5 show both the in cache and out of cache performance using the *No Flush* and *MultCallFlushLRU* strategies as presented in [1, 16]. Since an algorithm using *TT* kernels will need to call *GEQRT* as well as *TTQRT* to achieve the same as the *TS* kernel *TSQRT*, the comparison is made between *GEQRT* + *TTQRT* and *TSQRT* (and similarly for the updates). For  $n_b = 200$ , the observed ratio for in cache kernel speed for *TSQRT* to *GEQRT* + *TTQRT* is 1.3374, and for *TSMQR* to *UNMQR* + *TTMQR* is 1.3207. For out of cache, the ratio for *TSQRT* to *GEQRT* + *TTQRT* is 1.3193 and for *TSMQR* to *UNMQR* + *TTMQR* it is 1.3032. Thus, we can expect about a 30% difference between the selection of the kernels, since we will have instances of using in cache and out of cache throughout the run. Most of this difference is due to the higher efficiency and data locality within the *TT* kernels as compared to the *TS* kernels.

Having seen that kernel performance can have a significant impact, we also compare the *TT* based algorithms to those using the *TS* kernels. The goal is to provide a complete assessment of all currently available algorithms, as shown in Figure 6. For double precision, the observed difference in kernel speed is 4.976 GFLOP/sec for the *TS* kernels versus 3.844 GFLOP/sec for the *TT* kernels which provides a ratio of 1.2945 and is in accordance with our previous analysis. It can be seen that as the number of columns increases, whereby the amount of parallelism increases, the effect of the kernel performance outweighs the benefit provided by the extra parallelism afforded through the *TT* algo-

<sup>3</sup>When  $q = 1$ , GREEDY and FLATTREE exhibit close performance. They both perform a binary tree reduction, albeit with different row pairings.

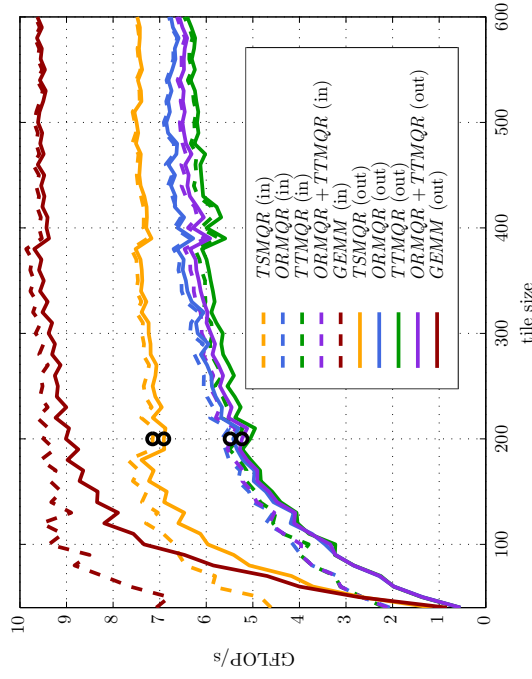
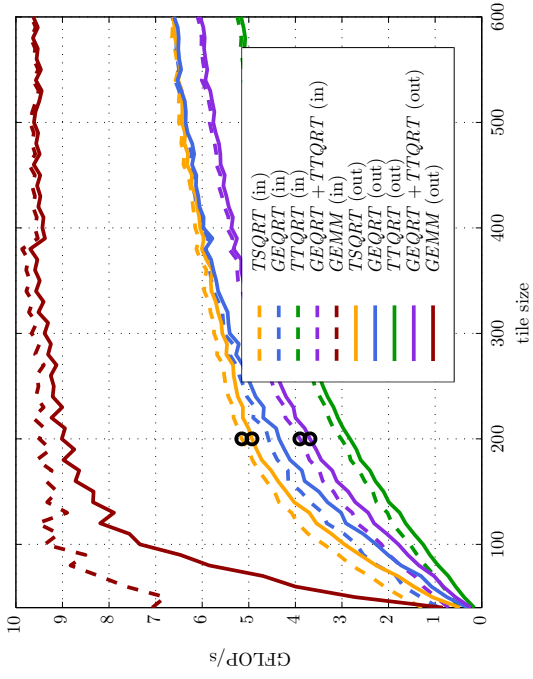


Figure 5: Kernel performance for double precision

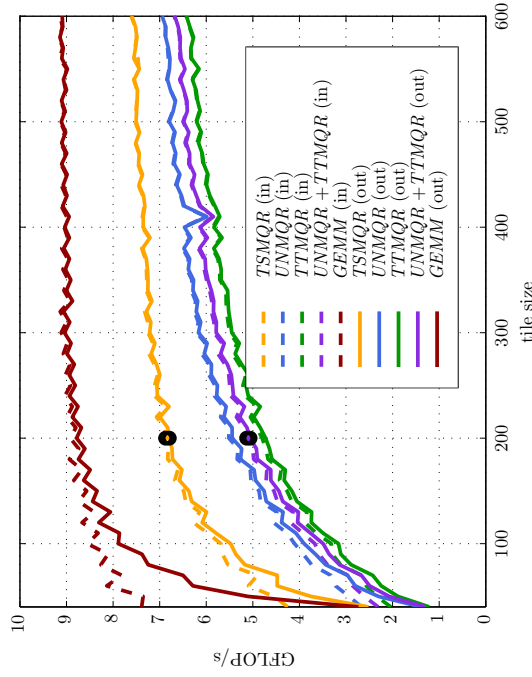
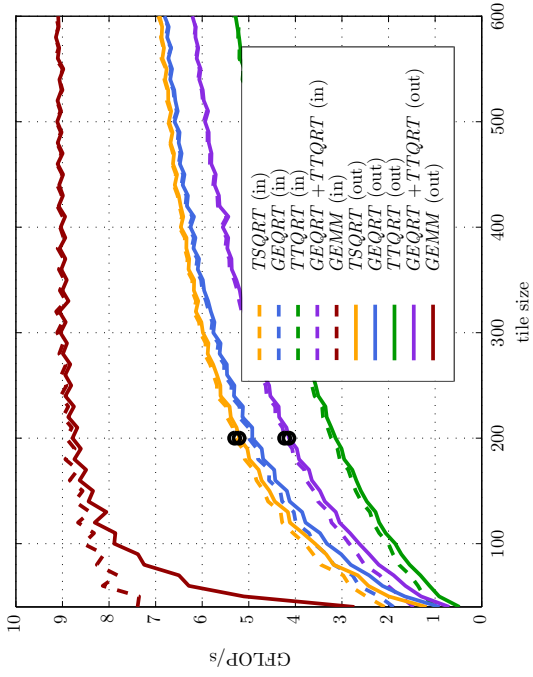
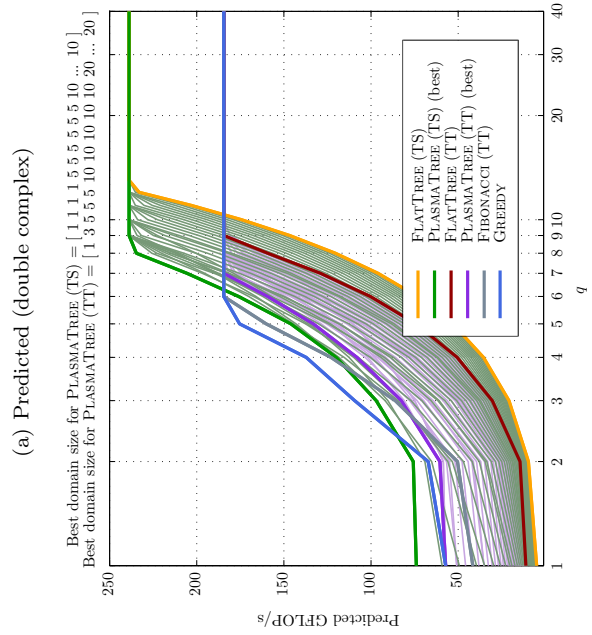
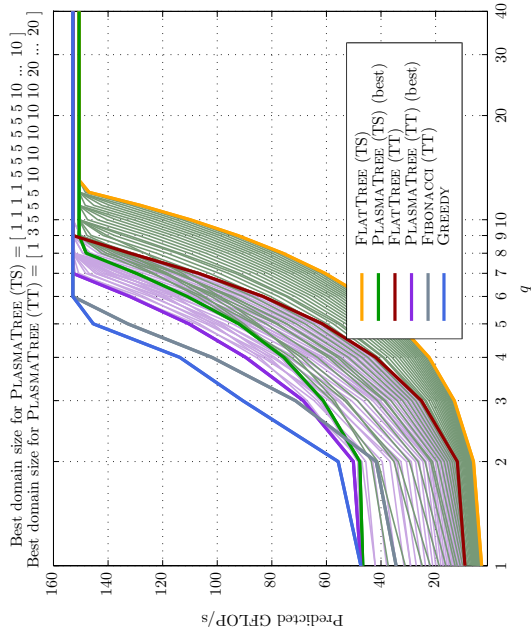
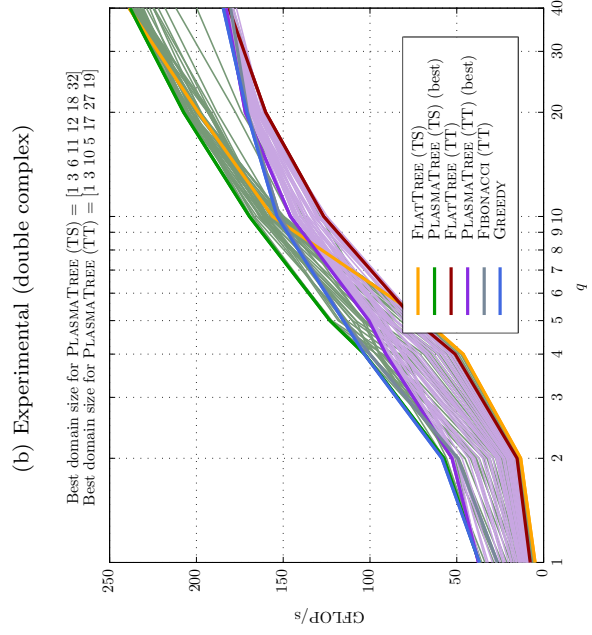
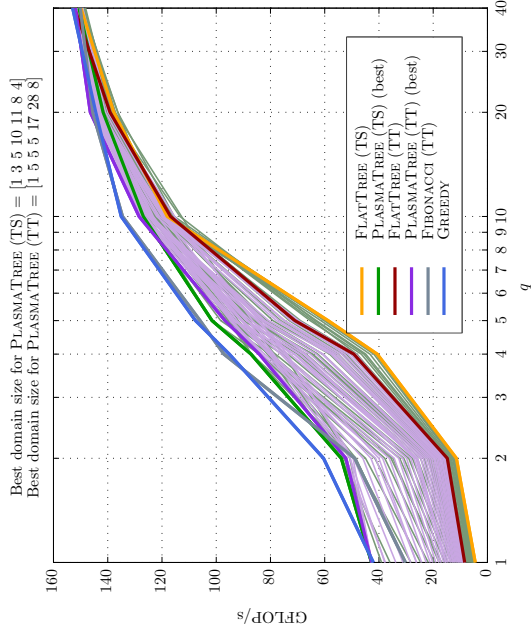


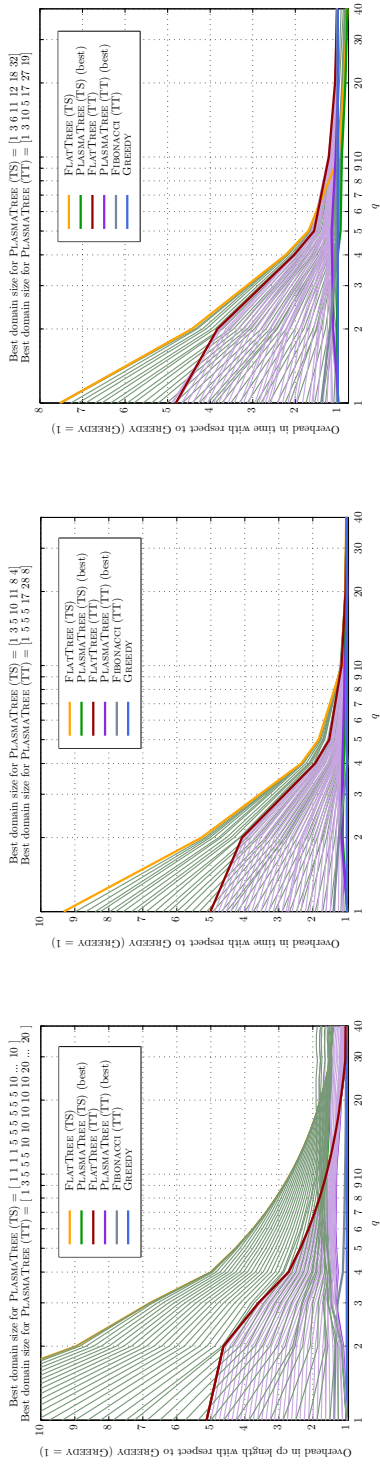
Figure 4: Kernel performance for double complex precision



(a) Predicted (double complex) (b) Experimental (double complex) (c) Predicted (double) (d) Experimental (double)

Figure 6: Predicted and experimental performance of QR factorization - All kernels



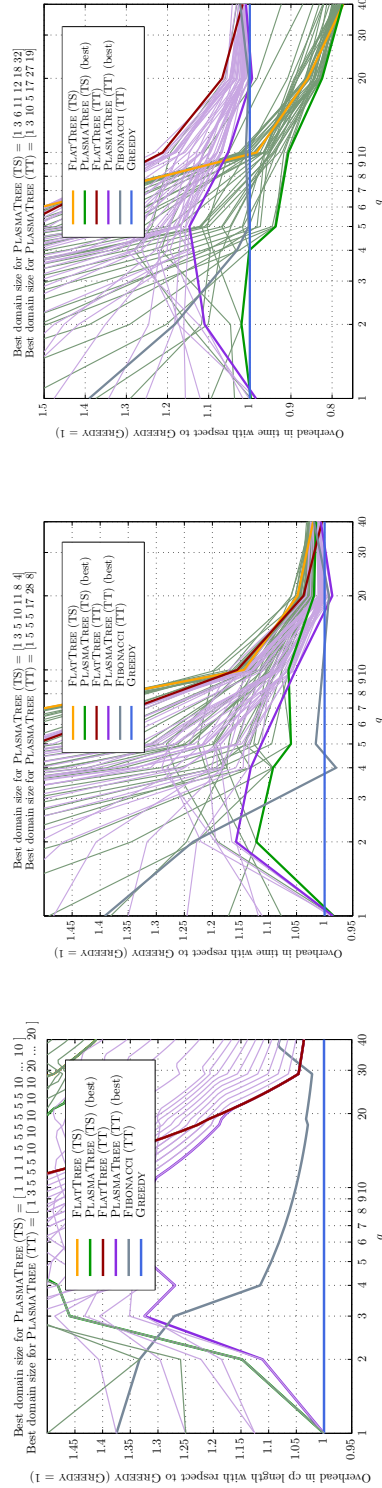


(a) Theoretical CP length

(b) Experimental (double complex)

(c) Experimental (double)

Figure 7: Overhead in terms of critical path length and time with respect to GREEDY (GREEDY = 1)



(a) Theoretical CP length

(b) Experimental (double complex)

(c) Experimental (double)

Figure 8: Detailed view of the overhead in terms of critical path length and time with respect to GREEDY (GREEDY = 1)

| $p$ | $q$ | GREEDY | PLASMATREE (TT) | BS | Overhead | Gain   | FIBONACCI | Overhead | Gain   |
|-----|-----|--------|-----------------|----|----------|--------|-----------|----------|--------|
| 40  | 1   | 16     | 16              | 1  | 1.0000   | 0.0000 | 22        | 1.3750   | 0.2727 |
| 40  | 2   | 54     | 60              | 3  | 1.1111   | 0.1000 | 72        | 1.3333   | 0.2500 |
| 40  | 3   | 74     | 98              | 5  | 1.3243   | 0.2449 | 94        | 1.2703   | 0.2128 |
| 40  | 4   | 104    | 132             | 5  | 1.2692   | 0.2121 | 116       | 1.1154   | 0.1034 |
| 40  | 5   | 126    | 166             | 5  | 1.3175   | 0.2410 | 138       | 1.0952   | 0.0870 |
| 40  | 6   | 148    | 198             | 10 | 1.3378   | 0.2525 | 160       | 1.0811   | 0.0750 |
| 40  | 7   | 170    | 226             | 10 | 1.3294   | 0.2478 | 182       | 1.0706   | 0.0659 |
| 40  | 8   | 192    | 254             | 10 | 1.3229   | 0.2441 | 204       | 1.0625   | 0.0588 |
| 40  | 9   | 214    | 282             | 10 | 1.3178   | 0.2411 | 226       | 1.0561   | 0.0531 |
| 40  | 10  | 236    | 310             | 10 | 1.3136   | 0.2387 | 248       | 1.0508   | 0.0484 |
| 40  | 11  | 258    | 336             | 20 | 1.3023   | 0.2321 | 270       | 1.0465   | 0.0444 |
| 40  | 12  | 280    | 358             | 20 | 1.2786   | 0.2179 | 292       | 1.0429   | 0.0411 |
| 40  | 13  | 302    | 380             | 20 | 1.2583   | 0.2053 | 314       | 1.0397   | 0.0382 |
| 40  | 14  | 324    | 402             | 20 | 1.2407   | 0.1940 | 336       | 1.0370   | 0.0357 |
| 40  | 15  | 346    | 424             | 20 | 1.2254   | 0.1840 | 358       | 1.0347   | 0.0335 |
| 40  | 16  | 368    | 446             | 20 | 1.2120   | 0.1749 | 380       | 1.0326   | 0.0316 |
| 40  | 17  | 390    | 468             | 20 | 1.2000   | 0.1667 | 402       | 1.0308   | 0.0299 |
| 40  | 18  | 412    | 490             | 20 | 1.1893   | 0.1592 | 424       | 1.0291   | 0.0283 |
| 40  | 19  | 432    | 512             | 20 | 1.1852   | 0.1562 | 446       | 1.0324   | 0.0314 |
| 40  | 20  | 454    | 534             | 20 | 1.1762   | 0.1498 | 468       | 1.0308   | 0.0299 |
| 40  | 21  | 476    | 554             | 20 | 1.1639   | 0.1408 | 490       | 1.0294   | 0.0286 |
| 40  | 22  | 498    | 570             | 20 | 1.1446   | 0.1263 | 512       | 1.0281   | 0.0273 |
| 40  | 23  | 520    | 586             | 20 | 1.1269   | 0.1126 | 534       | 1.0269   | 0.0262 |
| 40  | 24  | 542    | 602             | 20 | 1.1107   | 0.0997 | 556       | 1.0258   | 0.0252 |
| 40  | 25  | 564    | 618             | 20 | 1.0957   | 0.0874 | 578       | 1.0248   | 0.0242 |
| 40  | 26  | 586    | 634             | 20 | 1.0819   | 0.0757 | 600       | 1.0239   | 0.0233 |
| 40  | 27  | 608    | 650             | 20 | 1.0691   | 0.0646 | 622       | 1.0230   | 0.0225 |
| 40  | 28  | 630    | 666             | 20 | 1.0571   | 0.0541 | 644       | 1.0222   | 0.0217 |
| 40  | 29  | 652    | 682             | 20 | 1.0460   | 0.0440 | 666       | 1.0215   | 0.0210 |
| 40  | 30  | 668    | 698             | 20 | 1.0449   | 0.0430 | 688       | 1.0299   | 0.0291 |
| 40  | 31  | 684    | 714             | 20 | 1.0439   | 0.0420 | 710       | 1.0380   | 0.0366 |
| 40  | 32  | 700    | 730             | 20 | 1.0429   | 0.0411 | 732       | 1.0457   | 0.0437 |
| 40  | 33  | 716    | 746             | 20 | 1.0419   | 0.0402 | 754       | 1.0531   | 0.0504 |
| 40  | 34  | 732    | 762             | 20 | 1.0410   | 0.0394 | 776       | 1.0601   | 0.0567 |
| 40  | 35  | 748    | 778             | 20 | 1.0401   | 0.0386 | 798       | 1.0668   | 0.0627 |
| 40  | 36  | 764    | 794             | 20 | 1.0393   | 0.0378 | 820       | 1.0733   | 0.0683 |
| 40  | 37  | 780    | 810             | 20 | 1.0385   | 0.0370 | 842       | 1.0795   | 0.0736 |
| 40  | 38  | 796    | 826             | 20 | 1.0377   | 0.0363 | 862       | 1.0829   | 0.0766 |
| 40  | 39  | 812    | 842             | 20 | 1.0369   | 0.0356 | 878       | 1.0813   | 0.0752 |
| 40  | 40  | 826    | 856             | 20 | 1.0363   | 0.0350 | 892       | 1.0799   | 0.0740 |

Table 5: GREEDY versus PLASMATREE (TT) and FIBONACCI (Theoretical)

gorithms. Comparatively, in double complex precision, GREEDY does perform better, even against the algorithms using the  $TS$  kernels. As before, one must keep in mind that GREEDY does not require the tuning parameter of the domain size to achieve this better performance.

From these experiments, we showed that in double complex precision, GREEDY demonstrated better performance than any of the other algorithms and moreover, it does so without the need to specify a domain size as opposed to the algorithms in PLASMA. In addition, in double precision, for matrices where  $p \gg q$ , GREEDY continues to excel over any other algorithm using the  $TT$  kernels, and continues to do so as the matrices become more square.

## 5 Conclusion

In this paper, we have presented FIBONACCI, and GREEDY, two new algorithms for tiled QR factorization. These algorithms exhibit more parallelism than state-of-the-art implementations based on reduction trees. We have provided accurate

| $p$ | $q$ | GREEDY   | PLASMATREE (TT) | BS | Overhead | Gain    |
|-----|-----|----------|-----------------|----|----------|---------|
| 40  | 1   | 36.9360  | 37.5020         | 1  | 1.0153   | -0.0153 |
| 40  | 2   | 58.5090  | 52.7180         | 3  | 0.9010   | 0.0990  |
| 40  | 4   | 103.2670 | 90.7940         | 10 | 0.8792   | 0.1208  |
| 40  | 5   | 115.3060 | 100.5540        | 5  | 0.8721   | 0.1279  |
| 40  | 10  | 153.5180 | 145.8200        | 17 | 0.9499   | 0.0501  |
| 40  | 20  | 170.8730 | 171.8270        | 27 | 1.0056   | -0.0056 |
| 40  | 40  | 184.5220 | 182.8160        | 19 | 0.9908   | 0.0092  |

Table 6: GREEDY versus PLASMATREE (TT) (Experimenta Double)

| $p$ | $q$ | GREEDY   | PLASMATREE (TT) | BS | Overhead | Gain    |
|-----|-----|----------|-----------------|----|----------|---------|
| 40  | 1   | 42.0710  | 42.7120         | 1  | 1.0152   | -0.0152 |
| 40  | 2   | 60.4420  | 52.1970         | 5  | 0.8636   | 0.1364  |
| 40  | 4   | 95.1820  | 84.1120         | 5  | 0.8837   | 0.1163  |
| 40  | 5   | 107.6370 | 96.7530         | 5  | 0.8989   | 0.1011  |
| 40  | 10  | 135.0270 | 128.4320        | 17 | 0.9512   | 0.0488  |
| 40  | 20  | 144.4010 | 146.4220        | 28 | 1.0140   | -0.0140 |
| 40  | 40  | 152.9280 | 151.9090        | 8  | 0.9933   | 0.0067  |

Table 7: GREEDY versus PLASMATREE (TT) (Experimental Double Complex)

| $p$ | $q$ | GREEDY   | FIBONACCI | Overhead | Gain   |
|-----|-----|----------|-----------|----------|--------|
| 40  | 1   | 36.9360  | 26.5610   | 0.7191   | 0.2809 |
| 40  | 2   | 58.5090  | 49.4870   | 0.8458   | 0.1542 |
| 40  | 4   | 103.2670 | 100.1440  | 0.9698   | 0.0302 |
| 40  | 5   | 115.3060 | 115.0020  | 0.9974   | 0.0026 |
| 40  | 10  | 153.5180 | 152.0090  | 0.9902   | 0.0098 |
| 40  | 20  | 170.8730 | 170.4780  | 0.9977   | 0.0023 |
| 40  | 40  | 184.5220 | 180.2990  | 0.9771   | 0.0229 |

Table 8: Greedy versus FIBONACCI (Experimental Double)

| $p$ | $q$ | GREEDY   | FIBONACCI | Overhead | Gain    |
|-----|-----|----------|-----------|----------|---------|
| 40  | 1   | 42.0710  | 30.2280   | 0.7185   | 0.2815  |
| 40  | 2   | 60.4420  | 48.9570   | 0.8100   | 0.1900  |
| 40  | 4   | 95.1820  | 97.1650   | 1.0208   | -0.0208 |
| 40  | 5   | 107.6370 | 105.9610  | 0.9844   | 0.0156  |
| 40  | 10  | 135.0270 | 134.5500  | 0.9965   | 0.0035  |
| 40  | 20  | 144.4010 | 145.5530  | 1.0080   | -0.0080 |
| 40  | 40  | 152.9280 | 150.0980  | 0.9815   | 0.0185  |

Table 9: GREEDY versus FIBONACCI (Experimental Double Complex)

estimations for the length of their critical path, and we have proven that they were asymptotically optimal for a wide class of matrix shapes, including all cases where the number of tile rows  $p$  and tile columns  $q$  are proportional,  $p = \lambda q$ ,  $\lambda \geq 1$ . To the best of our knowledge, this proof is the first complexity result in the field of tiled algorithms, and it lays the theoretical foundations for a comparative study of these algorithms.

Comprehensive experiments on multicore platforms confirm the superiority of the new algorithms for  $p \times q$  matrices, as soon as, say,  $p \geq 2q$ . This holds true when comparing not only with previous algorithms using TT (*Triangle on top of triangle*) kernels, but also with all known algorithms based on TS (*Triangle on top of square*) kernels. Given that TS kernels offer more locality, and benefit from better elementary arithmetic performance, than TT kernels, the better performance of the new algorithms is even more striking, and further demonstrates that a large degree of a parallelism was not exploited in previously published solutions.

Future work will investigate several promising directions. First, using rectangular tiles instead of square tiles could lead to efficient algorithms, with more locality and still the same potential for parallelism. Second, refining the model to account for communications, and extending it to fully distributed architectures, would lay the ground to the design of MPI implementations of the new algorithms, unleashing their high level of performance on larger platforms. Finally, the design of robust algorithms, capable of achieving efficient performance despite variations in processor speeds, or even resource failures, is a challenging but crucial task to fully benefit from future platforms with a huge number of cores.

## References

- [1] E. Agullo, J. Dongarra, R. Nath, and S. Tomov. A fully empirical autotuned dense QR factorization for multicore architectures. Technical Report 242, LAPACK Working Note, 2011.
- [2] E. Agullo, B. Hadri, H. Ltaief, and J. Dongarra. Comparative study of one-sided factorizations with multiple software packages on multi-core hardware. In *Proceedings of the Conference on High Performance Computing Networking, Storage and Analysis (SC '09)*, pages 1–12. IEEE Computer Society Press, 2009.
- [3] S. Blackford and J. J. Dongarra. Installation guide for LAPACK. Technical Report 41, LAPACK Working Note, June 1999. originally released March 1992.
- [4] A. Buttari, J. Langou, J. Kurzak, and J. Dongarra. Parallel tiled QR factorization for multicore architectures. *Concurrency Computat.: Pract. Exper.*, 20(13):1573–1590, 2008.
- [5] A. Buttari, J. Langou, J. Kurzak, and J. Dongarra. A class of parallel tiled linear algebra algorithms for multicore architectures. *Parallel Computing*, 35(1):38–53, 2009.

- 
- [6] M. Cosnard, J.-M. Muller, and Y. Robert. Parallel QR decomposition of a rectangular matrix. *Numerische Mathematik*, 48:239–249, 1986.
- [7] M. Cosnard and Y. Robert. Complexity of parallel QR factorization. *Journal of the A.C.M.*, 33(4):712–723, 1986.
- [8] J. W. Demmel, L. Grigori, M. Hoemmen, and J. Langou. Communication-avoiding parallel and sequential QR and LU factorizations: theory and practice. Technical Report 204, LAPACK Working Note, 2008.
- [9] B. Hadri, H. Ltaief, E. Agullo, and J. Dongarra. Enhancing parallelism of tile QR factorization for multicore architectures. Technical Report 222, LAPACK Working Note, 2009.
- [10] B. Hadri, H. Ltaief, E. Agullo, and J. Dongarra. Tile QR factorization with parallel panel processing for multicore architectures. In *IPDPS'10, the 24th IEEE Int. Parallel and Distributed Processing Symposium*, 2010.
- [11] J. Kurzak, H. Ltaief, J. Dongarra, and R. M. Badia. Scheduling dense linear algebra operations on multicore processors. *Concurrency and Computation: Practice and Experience*, 22(1):15–44, 2010.
- [12] J. Modi and M. Clarke. An alternative Givens ordering. *Numerische Mathematik*, 43:83–90, 1984.
- [13] G. Quintana-Ortí, E. S. Quintana-Ortí, R. A. van de Geijn, F. G. V. Zee, and E. Chan. Programming matrix algorithms-by-blocks for thread-level parallelism. *ACM Transactions on Mathematical Software*, 36(3), 2009.
- [14] A. Sameh and D. Kuck. On stable parallel linear systems solvers. *J. ACM*, 25:81–91, 1978.
- [15] SimGrid. URL: <http://simgrid.gforge.inria.fr>.
- [16] R. C. Whaley and A. M. Castaldo. Achieving accurate and context-sensitive timing for code optimization. *Softw. Pract. Exper.*, 38:1621–1642, December 2008.
- [17] S. Williams, A. Waterman, and D. Patterson. Roofline: an insightful visual performance model for multicore architectures. *Commun. ACM*, 52:65–76, April 2009.



---

Centre de recherche INRIA Grenoble – Rhône-Alpes  
655, avenue de l'Europe - 38334 Montbonnot Saint-Ismier (France)

Centre de recherche INRIA Bordeaux – Sud Ouest : Domaine Universitaire - 351, cours de la Libération - 33405 Talence Cedex  
Centre de recherche INRIA Lille – Nord Europe : Parc Scientifique de la Haute Borne - 40, avenue Halley - 59650 Villeneuve d'Ascq  
Centre de recherche INRIA Nancy – Grand Est : LORIA, Technopôle de Nancy-Brabois - Campus scientifique  
615, rue du Jardin Botanique - BP 101 - 54602 Villers-lès-Nancy Cedex  
Centre de recherche INRIA Paris – Rocquencourt : Domaine de Voluceau - Rocquencourt - BP 105 - 78153 Le Chesnay Cedex  
Centre de recherche INRIA Rennes – Bretagne Atlantique : IRISA, Campus universitaire de Beaulieu - 35042 Rennes Cedex  
Centre de recherche INRIA Saclay – Île-de-France : Parc Orsay Université - ZAC des Vignes : 4, rue Jacques Monod - 91893 Orsay Cedex  
Centre de recherche INRIA Sophia Antipolis – Méditerranée : 2004, route des Lucioles - BP 93 - 06902 Sophia Antipolis Cedex

---

Éditeur  
INRIA - Domaine de Voluceau - Rocquencourt, BP 105 - 78153 Le Chesnay Cedex (France)  
<http://www.inria.fr>  
ISSN 0249-6399